ACS Macro Letters

Letter

pubs.acs.org/macroletters

Ionic Stabilization of the Polythiophene-Oxygen Charge-Transfer Complex

Christopher D. Weber, Stephen G. Robinson, David P. Stay, Chris L. Vonnegut, and Mark C. Lonergan*

Department of Chemistry and The Materials Science Institute, University of Oregon, Eugene, Oregon 97403, United States

Supporting Information

ABSTRACT: A substantial reduction in the rate of irreversible polymer photo-oxidation was observed through the ionic stabilization of the polymer-O_2 charge-transfer complex (CTC) in amorphous polythiophene thin films. Through the incorporation of anionic functionality containing mobile cations, it was found that CTC stability increases with increasing cation charge density. This results in an increased rate of electron transfer to molecular oxygen relative to photosensitization and reaction of $^1O_2$, leading to a reduction in the overall rate of polymer degradation. UV−vis and FTIR spectroscopy were utilized to determine the identity of intermediate and irreversible photodegradation products as well as the effect of ion identity on the dominant photo-oxidation mechanism. As polymer-O_2 CTCs are common in the photo-oxidation of many conjugated polymers, these results have significant implications for the ongoing effort to produce commercially viable organic electronic and photonic devices.

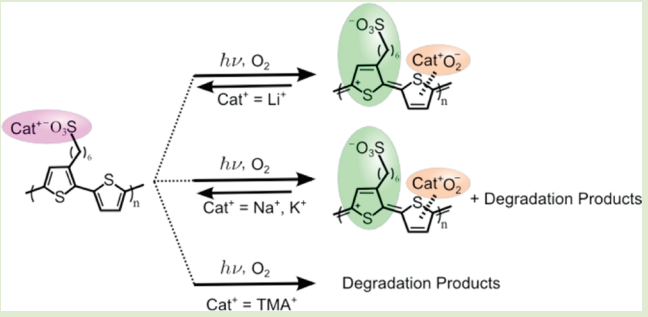

The application of conjugated polymers in practical photonic and electronic devices continues to be strongly inhibited by the inherent vulnerability of these materials to photo-oxidation.[1−7] Of particular interest among this class of materials are poly(3-alkylthiophene)s and other polythiophene derivatives, which are used as donor materials in bulk heterojunction organic photovoltaics (OPVs). Although much debate remains over the precise mechanisms that lead to irreversible polymer photodegradation, the formation of metastable charge-transfer complexes (CTCs) resulting from photoinduced electron transfer from the polymer to molecular oxygen ($P^+O_2^-$) are common to many of the proposed mechanisms.[8−14] The significance of these CTCs is that their presence is believed to reduce the rate of overall irreversible polymer degradation through the prevention or inhibition of follow-on reactions or alternate degradation pathways.[3,10,11,14] The inhibition of irreversible polymer degradation through the formation of a polymer-acceptor CTC has previously been demonstrated by incorporating stable electron acceptors, such as fullerenes or other small molecules such as 2,4,7-trinitrofluorenone;[15−17] however, efforts to reduce the rate of irreversible polymer photodegradation through the stabilization of the polymer-O_2 CTC have only recently been explored by our group.[18]

In this letter, we report the substantial influence of ionic interactions on the stability of the polythiophene-O_2 CTC and the corresponding inhibition of irreversible polymer degradation in amorphous polythiophene thin films. Through the incorporation of anionic functional groups containing mobile cations, we demonstrate that electrostatic stabilization of the polythiophene-O_2 CTC is directly correlated to the charge density of the mobile cation. By further elucidating the role of ionic functionality, we provide insight into the chemistry directing mechanistic pathways of photo-oxidation in conjugated polymers and provide a mechanistic explanation of the unusual photo-oxidative behavior observed in thin films of similar ionically functionalized polythiophenes as demonstrated by Arroyo-Villan et al. and others.[19,20]

To demonstrate the effect of ionic interactions on the photo-oxidation of polythiophene thin films, we utilized the conjugated polyelectrolyte (CPE) poly(6-(3-2,2′-bithienyl)-hexanesulfonate) with tetramethylammonium (TMAPT) or alkali metal (MPT, M = Li^+, Na^+, K^+) counterions (Chart 1).

Chart 1. Chemical Structure of Poly(6-(3-2,2′-bithienyl)-hexanesulfonate)

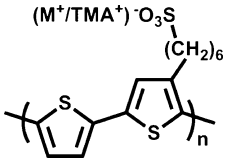

Thin films (30 nm) were exposed to long-term photo-oxidation (~8 days) under ambient laboratory conditions or to short-term accelerated photo-oxidation (40 min) using a high intensity tungsten light source (700−800 mW/cm^2) under

Received: January 23, 2012
Accepted: March 15, 2012
Published: March 23, 2012

low or high humidity oxygen (1 atm). FTIR spectroscopy of thick films (1−3 μm) was utilized to determine the identity of photo-oxidation intermediates and products in humidified oxygen using the same tungsten light source.

The effect of counterion charge density on overall polymer photo-oxidation under ambient conditions is shown in Figure 1.

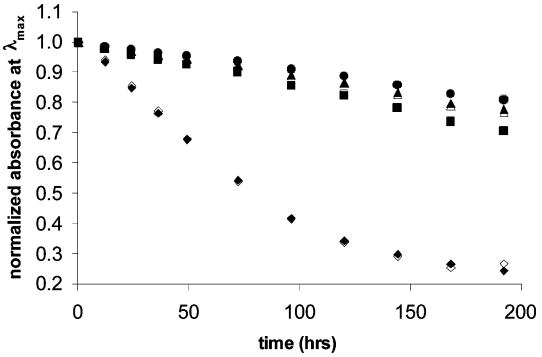

Figure 1. Normalized absorbance of thin films of LiPT (●), NaPT (▲), KPT (■), and TMAPT (♦) at 440 nm. The open and filled symbols represent two samples exposed to identical photo-oxidative conditions (~0.4 mW/cm^2). Film thicknesses were 30 nm.

The rate of photobleaching of the $\pi-\pi^*$ absorption at the initial λ_{max} is a commonly used metric for polymer photo-oxidation.[1,9,15,19] In this case, the rate is determined by the slope of the linear portion of the λ_{max} absorption as a function of time. A clear trend is observed between the rate of photobleaching and the charge density of the mobile counterion, with the overall rate increasing with decreasing counterion charge density. The salient feature of the photobleaching data is the large disparity of rates between the TMAPT and MPT films. The ratios of the ionic radii Li^+/K^+ and K^+/TMA^+ are both ~0.6; however, the rate of photobleaching increases by 50% between LiPT and KPT and by 320% between KPT and TMAPT films. Extensive blue shifting of the λ_{max} of TMAPT films is also observed on this time scale. The large disparity in rates suggests that counterion size alone is not the primary factor affecting the rate of photobleaching, but rather two different photo-oxidation mechanisms may exist, one dominating in the case of MPT films and another for TMAPT films. It is important to note that poly(3-hexylthiophene) (P3HT) thin films show an increase in photobleaching rate of 30% relative to TMAPT films. This suggests that anionic functionality, in general, has a stabilizing effect on polythiophene photo-oxidation.

To account for possible changes in film morphology due to counterion identity, atomic force microscopy (AFM) was used to verify that ion exchange does not alter the nanoscale morphology of the films (see Supporting Information). This, along with the lack of any significant differences in the initial absorbance spectra of the films, suggests that changes in polymer conformation are not the primary factor in the observed rates. Oxygen permeability is not believed to be a significant factor based on the reported oxygen diffusion coefficient for regiorandom P3HT thin films (1.2×10^{-8} cm^2 s^{-1}).[8] This results in an oxygen diffusion time of <1 ms for these film thicknesses.

Figure 2 shows the results of photo-oxidation of TMAPT and LiPT thin films under accelerated photo-oxidative conditions. The data show that the predominant photo-

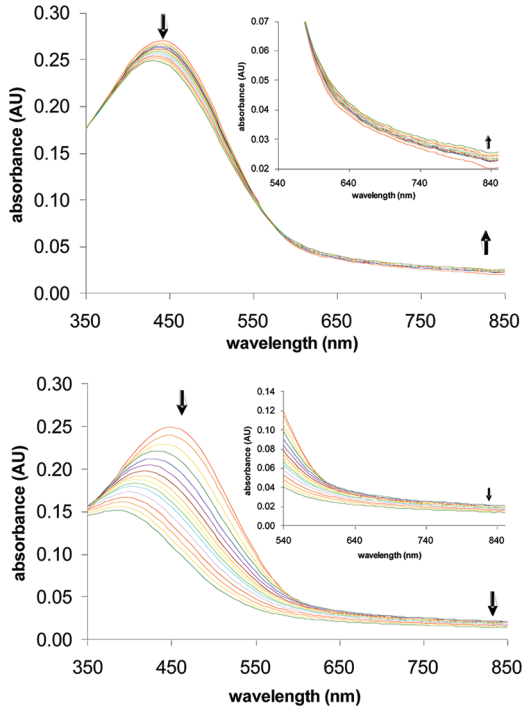

Figure 2. UV−vis spectra of initial photo-oxidation of LiPT (top) and TMAPT (bottom) films under oxygen atmosphere at 90 and 60% relative humidity, respectively (800 mW/cm^2). Spectra were collected every 2 min for the first 20, then every 4 min until 40 min total. Insets show the region between 540 and 850 nm. Arrows indicate the direction of the absorbance change in each region.

oxidative pathway differs based on the identity of the counterion. In the case of LiPT films, the decrease in the $\pi-\pi^*$ absorbance at 440 nm is accompanied by an increase in the vis-NIR absorbance between 600 and 850 nm, with a clear isosbestic point at ~550 nm. The decrease in the visible range and increase in the NIR are due to the formation of polaron (polymer radical cation) species on the polymer backbone resulting from electron transfer to oxygen (i.e., the formation of the polythiophene-O_2 CTC).[3,19,21,22] KPT films show the same behavior as LiPT films; however, the overall rate of photobleaching is greater than LiPT consistent with the data in Figure 1. In the case of TMAPT films, only a decrease of the $\pi-\pi^*$ absorbance and significant blue shifting of the visible transition is observed.

It has been suggested by Arroyo-Villan et al. in early studies of polythiophene CPE thin films that an increase in photo-oxidative stability may result from the increase in hydrophilicity imparted by ionic groups.[19] It was postulated that the increase in water content acted as a singlet oxygen ($^1O_2$) quencher based on the short $^1O_2$ lifetime in aqueous solution; however, the role played by $^1O_2$ in the solid state remains uncertain.[9] Our data show that the rate of photobleaching increases in all films with increasing humidity (see Supporting Information). It is important to note that in the case of MPT films, both the increase in the vis-NIR and decrease in the visible region are marginally accelerated in the presence of increased humidity; whereas, in the case of TMAPT films, only a dramatic decrease of the visible transition (with extensive blue shifting) is observed.

Figure 3 shows the FTIR spectra before and after photo-oxidation of a TMAPT film in the range of 1850−400 cm^{-1} (full spectra and intermediate times are shown in Supporting

dx.doi.org/10.1021/mz300046x | ACS Macro Lett. 2012, 1, 499−503

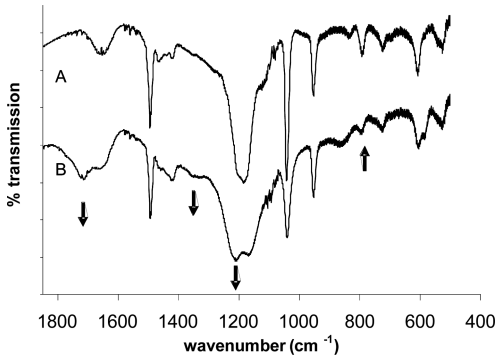

Figure 3. (A) Initial and (B) final (165 min) FTIR spectra of photo-oxidation of TMAPT film (2−3 μm thick) under oxygen atmosphere at 90% relative humidity (700 mW/cm^2). Arrows indicate direction of change and are discussed in the text. Spectra offset for clarity.

Information). The FTIR transmission (T) spectra of photo-oxidation products of TMAPT films are found to be in very good agreement with literature reports of the photo-oxidation of polythiophenes by a $^1O_2$ photo-oxidation mechanism.[23,24] The prominent bands at 1722, 1360, and 1213 cm^{-1} are assigned to C═O stretching, OH bending, and C═S$^+$O$^-$ or C═S═O stretching modes, respectively. Concomitant with the appearance of these bands is the decrease in C−H stretching modes in the range of 2800−3000 cm^{-1}, the aromatic C−H stretch at 3050 cm^{-1}, and C−H deformations at 800 cm^{-1}. The small initial band at 836 cm^{-1} is assigned to the O−O stretch of peroxide species and shifts to higher wavenumbers with time and broadens significantly. This broadening and shifting is likely due to the formation of various hydroperoxide and peroxide species in different chemical environments. Following photo-oxidation, TMAPT samples were placed in the dark under vacuum. No further spectral changes were observed after 2 days in vacuo indicating the formation of irreversible degradation products.

The difference spectra ($\Delta T = T(t) - T(t_{initial})$) for KPT and LiPT films in the range of 1850−400 cm^{-1} are shown in Figure 4 (full spectra shown in Supporting Information). The difference spectra allow for the resolution of specific bands that partially overlap with bands due to sulfonate stretches in the 1000−1250 cm^{-1} region. During photo-oxidation, several prominent bands appear in the FTIR difference spectra. These bands, located at 1333, 1140, 1060, and 1030 cm^{-1}, are assigned to oxygen doping (CTC formation) induced molecular vibrations associated with polarons on the polymer backbone, which are well documented.[25−27] Control doping experiments using I_2 vapor result in the appearance of identical bands (see Supporting Information). A broad absorbance tail in the region of 4000 cm^{-1} is also observed corresponding to the $D_1 \leftarrow D_0$ transition of the polymer radical cation.[3] The 1060 cm^{-1} band is not resolved in the case of LiPT due to the direct overlap with the SO_3^- symmetric stretch, which is shifted to higher energy due to the presence of the higher charge density Li^+ ion.[37] The prominent difference between the two films is the emergence of the 1722 cm^{-1} carbonyl band in the KPT films at 105 min. No resolvable peak at this wavenumber is seen in the LiPT spectra on this time scale. In fact, it takes more than 24 h of continuous irradiation for a small feature at 1722 cm^{-1} to be resolvable (see Supporting Information). Similar long-term photo-oxidations of KPT and LiPT reveal that the polaron band at 1333 cm^{-1} reaches a maximum at ∼2 h and

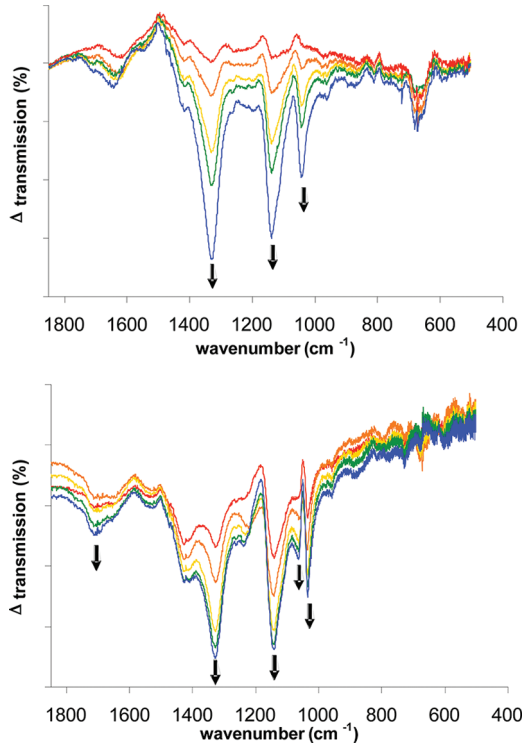

Figure 4. Difference FTIR spectra of LiPT (top) and KPT (bottom) films (1−2 μm thick) photo-oxidized under an oxygen atmosphere at 90% relative humidity (700 mW/cm^2). Plots represent 30 min increments from 45 min (red) to 165 min (blue). Arrows indicate direction of change and are discussed in the text.

does not decrease as the 1722 cm^{-1} carbonyl band grows into the spectrum. These data suggest that both irreversible degradation and electron transfer exist in parallel as suggested by other groups.[10,15,21] With continued irradiation (>48 h), the 1333 cm^{-1} band does begin to decrease in intensity possibly due to CTC dissociation, as suggested in the literature.[8,11,28] The peroxide O−O stretching mode at 836 cm^{-1} is observed in both KPT and LiPT films and does not broaden or shift as observed in the TMAPT films.

To ensure that oxygen permeability was not a factor using these thicker films, control experiments were conducted in which samples were exposed to wet oxygen overnight prior to illumination to allow full saturation of oxygen in the film. No effect on the rate of band formation is observed indicating rapid oxygen diffusion as estimated from the reported diffusion coefficient.

Following photo-oxidation, MPT samples were placed in the dark in either ambient conditions or in humid oxygen. Surprisingly, the doping induced infrared active bands all completely reverse within ∼1 h with no spectral changes associated with degradation observed (see Supporting Information). This is in stark contrast to reported photo-oxidations of P3HT thin films, which require vacuum, and often heating, to rapidly reverse oxygen doping.[3,13] Control experiments using regioregular P3HT were performed, and the oxygen doping induced IR bands remain observable for >1 week when stored under identical dark conditions. The mechanism of the rapid reversibility in MPT films is currently under investigation.

The data show the presence of two competing photo-oxidation mechanisms, the predominance of which depends

dx.doi.org/10.1021/mz300046x | ACS Macro Lett. 2012, 1, 499−503

upon the identity of the mobile counterion. At one extreme is the photosensitization and reaction of $^1O_2$. It is generally accepted that this is the dominant photo-oxidation mechanism in polythiophene solutions and likely in amorphous films as well,[9,21,23,29,30] although the latter has been questioned in recent work by Dupuis et al.[38] The formation of irreversible oxidation products observed in the FTIR spectra suggest that this is the dominant mechanism in the case of TMAPT films. The rapid rate of blue shifting and photobleaching observed in the UV−vis spectra of TMAPT films is also characteristic of the $^1O_2$ mechanism as reported by other groups studying the photo-oxidation of regiorandom P3HT films.[9] At the other extreme is the electron transfer mechanism forming a polythiophene-O_2 CTC. The observation of polaron infrared active vibrations and the lack of carbonyl oxidation products indicate that this is the dominant mechanism in LiPT films. The presence of both mechanisms seen in the KPT films by the appearance of both carbonyl degradation products and polarons in the FTIR spectra, as well as the increased rate of photobleaching relative to LiPT, suggests that a continuum exists in which the rate of electron transfer to oxygen, relative to photosensitization of $^1O_2$, can be correlated to the charge density of the mobile counterion. It is postulated that the rate of CTC formation is increased by the ability of the mobile high-charge-density cation and sulfonate group to effectively stabilize the negative and positive charges on the oxygen and polymer backbone, respectively, via Coulombic interactions. This synergistic ion stabilization of the polymer-O_2 CTC has also been seen in oxidation studies of anionically functionalized polyacetylenes.[18]

While it has been suggested that the presence of excess water acts to quench $^1O_2$,[19] the data presented here do not support this assertion. Zhou et al. has suggested that the presence of water in the photo-oxidation of P3HT films serves to solvate oxygen, effectively increasing its work function, facilitating electron transfer.[31] The results from the MPT photo-oxidation experiments in humid and dry conditions support this hypothesis; however, due to the hydrophilic nature of the films, it is possible that the presence of water also increases the mobility of both the polymer chains and mobile counterions, as seen in hydration studies of Nafion and other ionically functionalized polymer films.[32,33] This increased mobility would aid in the ability of the ion to take up the most advantageous position for ionic stabilization. This dependence of ion position on CTC stabilization has been demonstrated by numerous groups studying the photosensitization and reaction of $^1O_2$ with alkenes in NaY zeolite pores.[34−36] Our current work is focused on elucidating the molecular structure of the polythiophene-O_2 CTC and how specific ion interactions affect the rate of photo-oxidation.

We have demonstrated that ionic stabilization of the polythiophene-O_2 CTC in polythiophene films can dramatically affect the dominant photo-oxidation mechanism and substantially lower the rate of irreversible polymer degradation. The charge density of the mobile counterion has a direct influence on the rate of CTC formation with high-charge-density cations leading to increased rates of electron transfer to oxygen and lower rates of irreversible degradation due to $^1O_2$ photosensitization or other possible competing photodegradation mechanisms. The ability to inhibit degradation of conjugated polymers by incorporating electron acceptors of high electron affinity, such as fullerenes, has been demonstrated in the literature.[15] However, the ability to modulate the effective rates of photoinduced electron and energy transfer through the use of ionic functionality has not been previously explored. The results presented here have a direct impact on the ongoing debate regarding the precise photo-oxidation mechanism of P3HT films and devices. While several proposed mechanisms exist, including free radical mechanisms,[9,29] $^1O_2$ mechanisms,[10,21,23] and newer mechanisms involving polymer excited state reactions with ground state oxygen,[11] the common factor in these mechanisms is the formation of the polythiophene-O_2 CTC. Thus, the ability to stabilize the polythiophene-O_2 CTC results in increased inhibition of follow-on degradation reactions or alternate pathways. Inhibiting the rate of photo-oxidation of polythiophenes and other conjugated polymers is essential for their eventual use in practical devices such as OPVs. The ability to direct photochemical pathways through the use of ion stabilized intermediates opens new and exciting opportunities for the rational design of new materials with applications such as photocatalysis and oxygen reduction reactions.

EXPERIMENTAL SECTION

Polymer synthesis and characterization is described in the Supporting Information. Thin films of TMAPT were spun cast onto glass substrates from methanol solutions (∼20 mg/mL). Solid-state ion exchange was performed as described previously to prepare MPT films (M = Li^+, Na^+, K^+).[18] Thick films for FTIR analysis were drop cast onto silicon substrates from methanol or water for TMAPT and MPT (M = Li^+, K^+), respectively. All films were dried under vacuum for >12 h prior to analysis. For the long-term photo-oxidation studies, thin films were exposed to fluorescent lighting (∼0.4 mW/cm^2) under ambient laboratory conditions. For short-term accelerated photo-oxidation experiments, samples were placed in a custom designed chamber under vacuum. The chamber was backfilled with low or high humidity oxygen (1 atm). Humidity was determined using a Picotech humidity probe. Photo-oxidation was conducted using a tungsten light source at a distance of 12 in (∼800 mW/cm^2). UV−vis spectra were collected via optical windows on the chamber, which was mounted in the spectrometer using a custom mount. Photo-oxidations of thick films (1−3 μm) for FTIR were conducted in wet (RH 90%) oxygen in the same chamber at 1 atm and exposed to a tungsten light source at a distance of 10 in (∼700 mW/cm^2) for the specified time increments. Samples were removed briefly (5−10 min) to collect spectra.

ASSOCIATED CONTENT

Supporting Information

Polymer synthesis and characterization, XPS, AFM, low and high humidity UV−vis data, and FTIR spectra. This material is available free of charge via the Internet at http://pubs.acs.org.

AUTHOR INFORMATION

Corresponding Author

*E-mail: lonergan@uoregon.edu.

Notes

The authors declare no competing financial interest.

ACKNOWLEDGMENTS

This work was funded by the Division of Chemical Sciences, Geosciences, and Biosciences, Office of Basic Energy Sciences of the U.S. Department of Energy through Grant DE-FG02-07ER15907. This project made use of equipment in the SUNRISE Photovoltaic Laboratory supported by the Oregon Built Environment and Sustainable Technologies (BEST) signature research center. C.D.W. acknowledges support by the National Science Foundation IGERT program under Grant

No. DGE-0549503. The authors also acknowledge Diana Standish for the design and fabrication of optical mounts utilized in this work.

REFERENCES

(1) Jorgensen, M.; Norrman, K.; Krebs, F. C. *Sol. Energy Mater. Sol. Cells* **2008**, *92*, 686−714.
(2) Reese, M. O.; Nardes, A. M.; Rupert, B. L.; Larsen, R. E.; Olson, D. C.; Lloyd, M. T.; Shaheen, S. E.; Ginley, D. S.; Rumbles, G.; Kopidakis, N. *Adv. Funct. Mater.* **2010**, *20*, 3476−3483.
(3) Aguirre, A.; Meskers, S. C. J.; Janssen, R. A. J.; Egelhaaf, H. J. *Org. Electron.* **2011**, *12*, 1657−1662.
(4) Seemann, A.; Egelhaaf, H. J.; Brabec, C. J.; Hauch, J. A. *Org. Electron.* **2009**, *10*, 1424−1428.
(5) Lipson, S. M.; O'Brien, D. F.; Byrne, H. J.; Davey, A. P.; Blau, W. J. *Synth. Met.* **2000**, *111*, 553−557.
(6) Manceau, M.; Bundgaard, E.; Carle, J. E.; Hagemann, O.; Helgesen, M.; Sondergaard, R.; Jorgensen, M.; Krebs, F. C. *J. Mater. Chem.* **2011**, *21*, 4132−4141.
(7) Chandross, E. A. *Science* **2011**, *333*, 35−36.
(8) Abdou, M. S. A.; Orfino, F. P.; Son, Y.; Holdcroft, S. *J. Am. Chem. Soc.* **1997**, *119*, 4518−4524.
(9) Hintz, H.; Egelhaaf, H. J.; Luer, L.; Hauch, J.; Peisert, H.; Chasse, T. *Chem. Mater.* **2011**, *23*, 145−154.
(10) Sperlich, A.; Kraus, H.; Deibel, C.; Blok, H.; Schmidt, J.; Dyakonov, V. *J. Phys. Chem. B* **2011**, *115*, 13513−13532.
(11) Cook, S.; Furube, A.; Katoh, R. *J. Mater. Chem.* **2012**, *22*, 4282−4289.
(12) Hintz, H.; Peisert, H.; Egelhaaf, H. J.; Chasse, T. *J. Phys. Chem. C* **2011**, *115*, 13373−13376.
(13) Liao, H. H.; Yang, C. M.; Liu, C. C.; Horng, S. F.; Meng, H. F.; Shy, J. T. *J. Appl. Phys.* **2008**, *103*, 104506.
(14) Luer, L.; Egelhaaf, H. J.; Oelkrug, D.; Cerullo, G.; Lanzani, G.; Huisman, B. H.; de Leeuw, D. *Org. Electron.* **2004**, *5*, 83−89.
(15) Sarkas, H. W.; Kwan, W.; Flom, S. R.; Merritt, C. D.; Kafafi, Z. H. *J. Phys. Chem.* **1996**, *100*, 5169−5171.
(16) Golovnin, I. V.; Bakulin, A. A.; Zapunidy, S. A.; Nechvolodova, E. M.; Paraschuk, D. Y. *Appl. Phys. Lett.* **2008**, *92*, 243311.
(17) Chambon, S.; Rivaton, A.; Gardette, J.-L.; Firon, M. *Sol. Energy Mater. Sol. Cells* **2007**, *91*, 394−398.
(18) Weber, C. D.; Robinson, S. G.; Lonergan, M. C. *Macromolecules* **2011**, *44*, 4600−4604.
(19) Arroyo-Villan, M. I.; Diazquijada, G. A.; Abdou, M. S. A.; Holdcroft, S. *Macromolecules* **1995**, *28*, 975−984.
(20) Tran-Van, F.; Carrier, M.; Chevrot, C. *Synth. Met.* **2004**, *142*, 251−258.
(21) Koch, M.; Nicolaescu, R.; Kamat, P. V. *J. Phys. Chem. C* **2009**, *113*, 11507−11513.
(22) Yamamoto, T. *Chem. Lett.* **2003**, *32*, 334−335.
(23) Abdou, M. S. A.; Holdcroft, S. *Macromolecules* **1993**, *26*, 2954−2962.
(24) Holdcroft, S. *Macromolecules* **1991**, *24*, 4834−4838.
(25) Navarrete, J. T. L.; Zerbi, G. *J. Chem. Phys.* **1991**, *94*, 965−970.
(26) Moraes, F.; Schaffer, H.; Kobayashi, M.; Heeger, A. J.; Wudl, F. *Phys. Rev. B* **1984**, *30*, 2948−2950.
(27) Ivaska, A.; Osterholm, J. E.; Passiniemi, P.; Kuivalainen, P.; Isotalo, H.; Stubb, H. *Synth. Met.* **1987**, *21*, 215−221.
(28) Ogilby, P. R.; Kristiansen, M.; Clough, R. L. *Macromolecules* **1990**, *23*, 2698−2704.
(29) Manceau, M.; Rivaton, A.; Gardette, J. L.; Guillerez, S.; Lemaitre, N. *Polym. Degrad. Stab.* **2009**, *94*, 898−907.
(30) Osterbacka, R.; An, C. P.; Jiang, X. M.; Vardeny, Z. V. *Science* **2000**, *287*, 839−842.
(31) Zhuo, J. M.; Zhao, L. H.; Png, R. Q.; Wong, L. Y.; Chia, P. J.; Tang, J. C.; Sivaramakrishnan, S.; Zhou, M.; Ou, E. C. W.; Chua, S. J.; Sim, W. S.; Chua, L. L.; Ho, P. K. H. *Adv. Mater.* **2009**, *21*, 4747−4752.
(32) Kusoglu, A.; Modestino, M. A.; Hexemer, A.; Segalman, R. A.; Weber, A. Z. *ACS Macro Lett.* **2012**, *1*, 33−36.
(33) Freund, M. S.; Deore, B. *Self-Doped Conducting Polymers*; Wiley: West Sussex, England; Hoboken, NJ, 2006.
(34) Blatter, F.; Frei, H. *J. Am. Chem. Soc.* **1993**, *115*, 7501−7502.
(35) Robbins, R. J.; Ramamurthy, V. *Chem. Commun.* **1997**, 1071−1072.
(36) Clennan, E. L.; Pace, A. *Tetrahedron* **2005**, *61*, 6665−6691.
(37) Lowry, S. R.; Maurritz, K. A. *J. Am. Chem. Soc.* **1980**, *102*, 4665−4667.
(38) Dupuis, A.; Wong-Wah-Chung, P.; Rivaton, A.; Gardette, J.-L. *Polym. Degrad. Stab.* **2012**, *97*, 366−374.